5B.3

Global Climatology of Tropospheric CO from the Atmospheric InfraRed Sounder (AIRS)

W. Wallace McMillan[a], Leonid Yurganov[b], Keith Evans[b], and Chris Barnet[c]

[a]Department of Physics, University of Maryland, Baltimore County, 1000 Hilltop Circle, Baltimore, Maryland, 21250-0001 USA;

[b]Joint Center for Earth Systems Technology, University of Maryland, Baltimore County, 1000 Hilltop Circle, Baltimore, Maryland, 21250-0001 USA;

[c]Integrated Observing System Science and Product Development Team, NOAA/NESDIS/STAR E/RA1, 5200 Auth Road, Camp Springs, MD 20746;

ABSTRACT

Five years of CO retrievals from the Atmospheric InfraRed Sounder (AIRS) onboard NASA's Aqua satellite reveal variations in tropospheric CO on timescales from twelve hours to five years. The shorter timescales are invaluable to monitor daily variations in CO emissions, for three-dimensional tracking of atmospheric motions, and for insights into atmospheric mixing. Previous studies have utilized AIRS CO retrievals over the course of days to weeks to track plumes from large forest fires. Substantial interannual variations demonstrate year-to-year changes in rainfall and drought patterns in different seasons. We see such interannual variations in the biomass burning emissions from the Northern Hemisphere's boreal forests and South America, while industrial contributions are evident at smaller magnitudes on seasonal timescales. Variations on multi-year timescales exhibit the influence of large scale atmospheric perturbations including ENSO. In particular, we observe a quasi-biennial variation in CO emissions from Indonesia with varying magnitudes in peak emission occurring in 2002, 2004, and 2006. Examining satellite rainfall measurements over Indonesia, we find the enhanced CO emission correlates with occasions of less rainfall during the month of October. Unfortunately, neither AIRS nor MOPITT was in orbit during the ENSO year of 1997-1998 when Indonesia experienced horrendous fires. Continuing this satellite record of tropospheric CO with measurements from the European IASI instrument will permit construction of a long time-series useful for further investigations of climatological variations in CO emissions and their impact on the health of the atmosphere.

1. INTRODUCTION

With a capacity for daily global observations of numerous atmospheric parameters, NASA's Atmospheric InfraRed Sounder (AIRS) onboard the Aqua satellite provides a unique perspective of the Terrestrial troposphere.[1] These capabilities have been utilized in several recent NASA/International field experiments including the INtercontinental chemical Transport EXperiment–North America Phase A (INTEX-A) in July and August 2004,[2] INTEX-B March through May 2006, and the 2006 Texas Air Quality Study (TexAQSII) August through October 2006. AIRS observations of tropospheric carbon monoxide (CO) during INTEX-A illuminate several North American industrial and biomass burning sources and subsequent transport paths.[2–5] Similarly, AIRS CO observations over Europe and Asia document transport of European and Chinese biomass burning and industrial emissions to the Arctic.[6,7]

Further author information: (Send correspondence to W.W.M.)
W.W.M.: E-mail: mcmillan@umbc.edu, Telephone: 1 410 455 6315

CO surface concentrations have long been known to exhibit influences from distant sources based on chemical lifetime estimates,[8] in situ measurements and modeling[9,10] and studies of surface concentrations.[11,12] Over the past decade, the impacts of such long-range transport have become evident not only on the intercontinental scale but as hemispheric and potentially global phenomena.[13,14]

Satellite observations commencing with the Measurement of Air Pollution from Space (MAPS) instrument onboard the Space Shuttle in 1981 illustrated the global distribution of CO and large-scale biomass burning as a significant global CO source.[15,16] Since 2000, the wealth of CO retrievals from the Measurement Of Pollution In The Troposphere (MOPITT) instrument on NASA's Terra satellite have shown CO transport on time scales of several days.[17,18] Additionally, MOPITT has provided estimates of CO emissions from the 2004 Alaska/Canada fires[19–21] and explored correlations between CO signatures and aerosols.[22,23] Retrievals of tropospheric CO from airborne remote sensors have contributed to our appreciation of long range transport.[24–26] Other than AIRS, the most recent satellite instruments to measure tropospheric CO are the Tropospheric Emission Spectrometer (TES) onboard NASA's Aura satellite[27] and the Scanning Imaging Absorption Spectrometer for Atmospheric Chartography (SCIAMACHY) onboard the European Envisat satellite.[28]

Launched onboard NASA's Aqua satellite on 4 May 2002, AIRS cross-track scanning grating spectrometer coupled with Aqua's cross-track scanning Advanced Microwave Sounding Unit (AMSU) provide vertical profiles of the atmosphere with a nadir 45 km field-of-regard (FOR) across a 1650 km swath.[1,29] Designed as a prototype next generation temperature and water vapor sounder, AIRS broad spectral coverage (3.7 to 16 μm with 2378 channels) includes spectral features of O_3, CO_2, CH_4, and CO.[30] AIRS broad swath, infrared spectral coverage, and cloud-clearing[31] enable day/night retrievals over nearly 70% of the planet every day with substantial portions of the globe observed twice daily (ascending and descending orbits). Thus, AIRS readily observes global scale transport from large CO sources on at least daily time scales.[6,7,32]

With biomass burning and oxidation of naturally occurring volatile hydrocarbons accounting for nearly 50% of tropospheric CO,[8,9] monitoring changes in these sources, changes in anthropogenic sources, and subsequent transport is key to assessing the impact on tropospheric chemistry and near-surface air quality. CO's relatively long lifetime, on average one-half to three months in different portions of the troposphere, make it an excellent tracer of transport and source variability.[33] Increases in global tropospheric CO from 1970 to the late 1980s has been linked to increasing anthropogenic emissions.[34] Subsequent studies found global tropospheric CO abundances leveled off and began to decrease from 1990 to 2000 due to tighter controls on automobile emissions.[35] However, recent studies have postulated possible large scale increases and variations in biomass burning sources in the boreal region due to climate change.[36,37]

AIRS and its successor satellite instruments are uniquely capable to assess the global impact of such changes in sources and downwind transport. Similar to the instruments that preceeded AIRS to orbit, MAPS and MOPITT, AIRS' spectral resolution yields a CO sensitivity broadly peaking in the mid-troposphere (300 to 700 mb) with limited information on the vertical distribution. Thus, although AIRS readily detects CO, interpreting AIRS CO retrievals requires skill and caution. An observed increase in CO abundance by AIRS may indicate more CO is present (stronger source) or that the CO has been lifted into the mid-troposphere where AIRS is more sensitive. Typically, AIRS observes less CO enhancement near a source than downwind where it has been lifted above the boundary layer. However, under some conditions, AIRS can see CO down to at least the top of the boundary layer. Detailed validation studies of AIRS retrieved CO profiles and CO total column are underway with publication expected in early 2009.

2. AIRS CO RETRIEVALS

AIRS was designed as a prototype next generation atmospheric sounder for NASA and NOAA polar orbiting satellites.[1] As such, AIRS' performance was optimized to retrieve highly accurate temperature (1K RMS error in 1km tropospheric layers) and water vapor profiles (15% RMS error in 2 km tropospheric

layers).[1] In practice, AIRS temperature and water vapor retrievals exceed the target accuracy for cloud-free scenes[38] and are nominally less accurate for cloud-cleared scenes.[39] The full AIRS team retrieval algorithm is described in Susskind et al. [2003][31] which includes a detailed discussion of AIRS cloud-clearing, temperature, water vapor, and O_3 retrievals. The AIRS CO retrievals shown here were produced as operational products by the NASA Goddard Earth Sciences (GES) Data Information and Service Center (DISC) utilizing version 5.0.14.0 (hereafter v5) of the AIRS Team retrieval algorithm. Details of this latest version of the AIRS CO retrieval algorithm are available in Comer [2006].[40] The full five and one-half year record of AIRS data are now publicly available on the internet from the Goddard DISC (http://disc.gsfc.nasa.gov/AIRS/data_access.shtml).

As described by McMillan et al. [2005],[32] tropospheric CO abundances are retrieved from AIRS measured radiances in the 4.58-4.50 μm (2183-2220 cm^{-1}) region of the 1–0 vibration-rotation CO fundamental band through numerical inversion of the radiative transfer equation employing the AIRS fast forward radiative transfer model.[41] This fast model performs all computations on a set of 100 layers referred to as the AIRS standard layers.

The AIRS v5 CO retrieval algorithm utilizes a set of vertically overlapping trapezoidal functions determined from optimization studies comparing AIRS CO retrievals to in situ aircraft measurements.[40] The overall methodology of the AIRS CO retrieval algorithm is analogous to the AIRS O_3 retrieval algorithm.[31] Additional details of the methodology of the AIRS retrieval algorithm and development of the AIRS averaging kernels are described by Maddy et al. [2008].[42] The CO algorithm begins with a single fixed CO profile as its first guess. The previously mentioned optimization study[40] determined that the MOPITT a priori CO profile[17] was the best choice for a single global first guess profile for AIRS CO retrievals.

With similar sensitivity to mid-tropospheric CO as MAPS and MOPITT, AIRS' unique daily global view provides nearly ten times as many retrievals per day as MOPITT and enables process studies of phenomena on 12 to 24 hour time scales.[32] However, AIRS spectral resolution (nearly 2 cm^{-1} in the CO region) provides insufficient vertical information to uniquely constrain the CO profile. Thus, like MAPS and MOPITT, AIRS CO retrievals are sensitive to a weighted total column of tropospheric CO. In terms of the trapezoidal functions, a perturbation to one function is strongly correlated to perturbations of the other functions.

In more traditional numerical solutions to inverse problems, the vertical weighting of sensitivity is defined as the averaging kernel.[43] In such a formulation, (1 - averaging kernel) represents the amount of a priori remaining in the final retrieved solution. Although the AIRS team retrieval algorithm is not formulated as a maximum likelihood problem,[31,42] it does compute a quantity similar to an averaging kernel but in the reduced measurement space defined by the trapezoids. The 100 layer AIRS CO retrievals (column CO in each radiative transfer layer) are related to this reduced measurement space by a unitary transformation.[31] The AIRS algorithm employs a smoothness constraint by damping the least significant eigenvectors of the unitary transformation. The magnitude of this damping was determined in the optimization studies of Comer [2006].[40] Globally, v5 of the AIRS CO retrieval possesses 0.5 to 1.5 degrees of freedom (sum of the eigenvalues) and often, even the largest eigenvector is partially damped.[32]

With nine trapezoidal perturbation functions, the v5 AIRS CO retrieval algorithm produces a 9×9 matrix with each row corresponding to the averaging kernel for the respective trapezoid. Each averaging kernel represents the response of the retrieval to a perturbation in the respective trapezoid. Figure 1 presents two sets of averaging kernels, one for a relatively clean atmosphere over the central United States, and one with a polluted boundary layer containing industrial and biomass burning emissions. For the clean case, note how most of the averaging kernels have similar shapes and peak near 500 mb. For the polluted case, note how the averaging kernels for the two lowest trapezoids peak between 700 and 850 mb and at the surface are as significant as any other averaging kernel. Although the retrieval algorithm may underestimate boundary layer CO abundances, the averaging kernels indicate the radiances are providing meaningful information much closer to the surface than the nominal peak sensitivity at 500 mb.

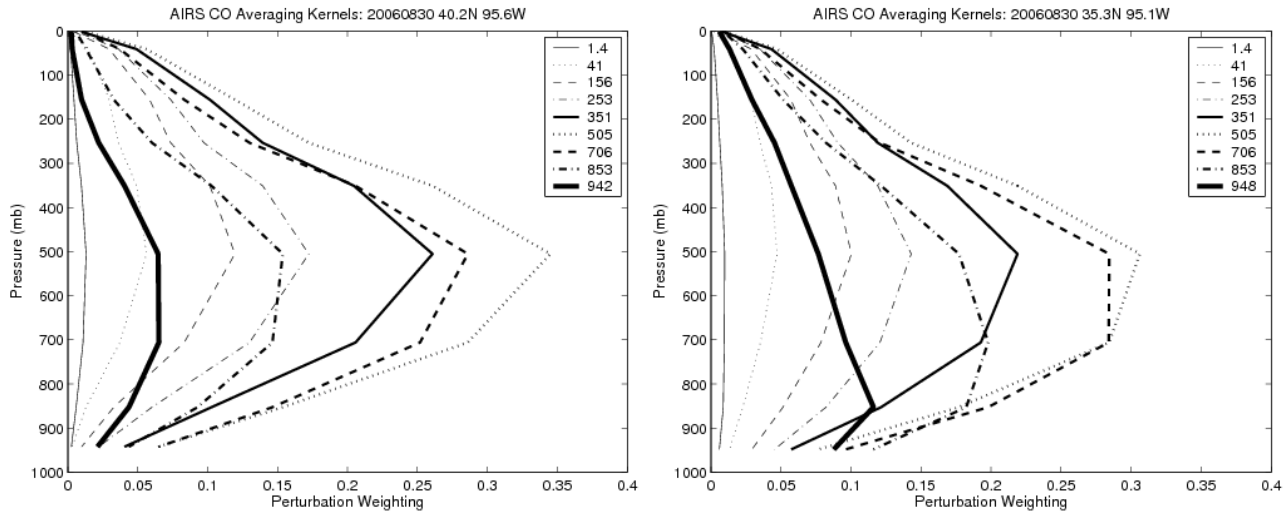

Figure 1. The left hand panel presents nominal AIRS CO averaging kernels for a clean atmosphere over the Central United States (40.2 N, 95.6 W) on 30 August 2006. On the right are AIRS CO averaging kernels for a scene with a polluted boundary layer over north Texas (35.3 N,95.1 W) on the same day. The numbers in the legend indicate the effective pressures of each of the nine AIRS trapezoidal perturbation functions.

3. DAILY CO MAPS

Figures 2 illustrate the extent of AIRS daily coverage of tropospheric CO at 500 mb, the nominal peak of AIRS vertical sensitivity and the magnitude of the seasonal variations in tropospheric CO. On 11 April 2007, note the inter-hemispheric difference with high values in the north and low values in the south. This seasonal dichotomy results primarily from the seasonal photochemical cycle of OH, the primary oxidizer for CO. The end of winter/early spring in the Northern Hemisphere coincides with the minimum of OH concentrations and thus a maximum for CO concentrations. Extensive sources are evident in both China and Southeast Asia with subsequent plumes transported eastward across the Pacific Ocean to North America. In contrast, the 19 October map is near the peak of the biomass burning seasons in South America and southern Africa and exhibits large CO abundances in the Southern Hemisphere and generally low CO abundances in the North. In the early fall for the Northern Hemisphere, OH abundance is near a maximum; CO is near its minimum. Again, long-range transport of CO is evident with biomass burning plumes from both South America and southern Africa nearly circling the globe with multiple rivers of smoke.[25,44] Studies of v4 AIRS retrievals for September 2002 previously documented such long-range transport from South American fires[32] and verified a new plume-rise model.[45] Additional detailed studies will yield a wealth of information about changing emission sources, vertical transport (including wildfire emission injection heights and boundary layer venting), and large-scale dynamics and mixing. Preliminary results of two studies are discussed further in the following two sections.

4. INTERANNUAL VARIATIONS AND MEGACITIES

Figure 3 illustrates the annual average distribution of CO for 2003. The local CO maximum just east of Lake Baikal occurs precisely in a region that experienced extensive biomass burning in 2003. In contrast, subsequent years show much less CO over eastern Siberia. Unfortunately, file size restrictions do not permit us to show more than one such map in this manuscript. Examination of the full record of AIRS CO retrievals reveals interannual variations over the Alaskan and Canadian Yukon (maximum in summer of 2004[2]) and over South America and Indonesia as discussed in more detail in the following section.

Looking carefully at Figure 3, two very localized areas stand out against their backgrounds: Mexico City (20N, 100W) and Tehran (35N, 50E, just south of the Caspian Sea). In fact, these two areas are evident in nearly all daily maps. A five-year timeseries of retrieved AIRS 500 mb CO for the two

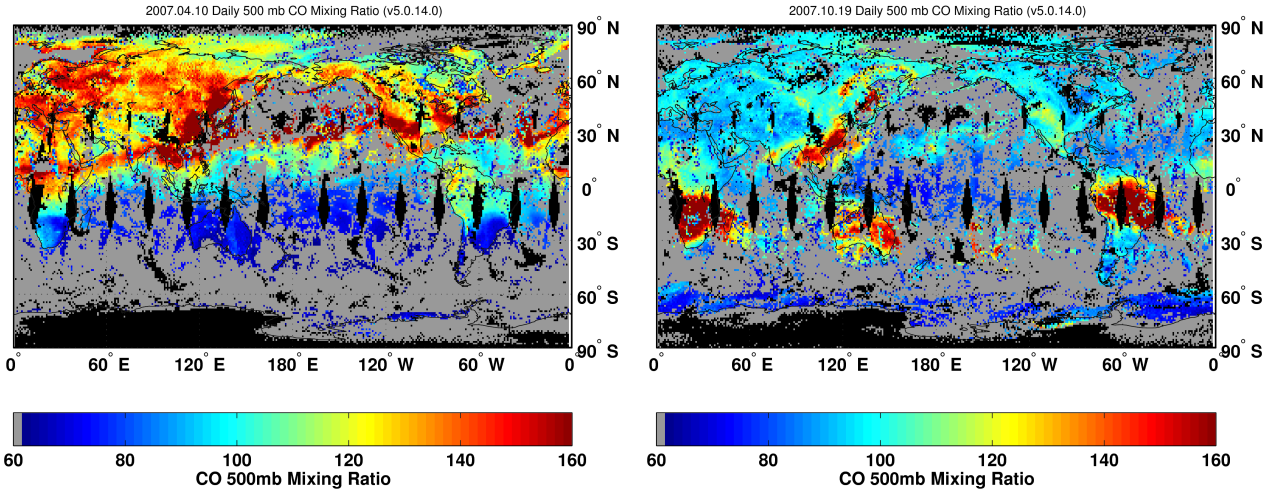

Figure 2. The left-hand map shows the distribution of 500 mb CO as retrieved by AIRS on 10 April 2007. The right-hand map shows the distribution six months later on 19 October 2007. Both maps are on 1 × 1 degree grids.

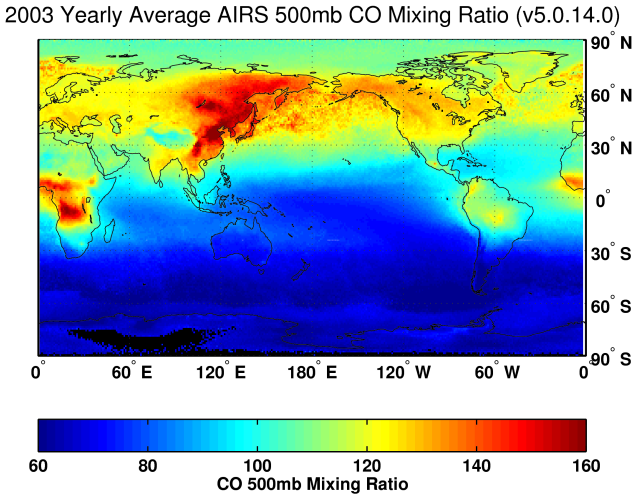

Figure 3. This map presents the 2003 yearly average distribution of 500 mb CO on a 1x1 degree grid.

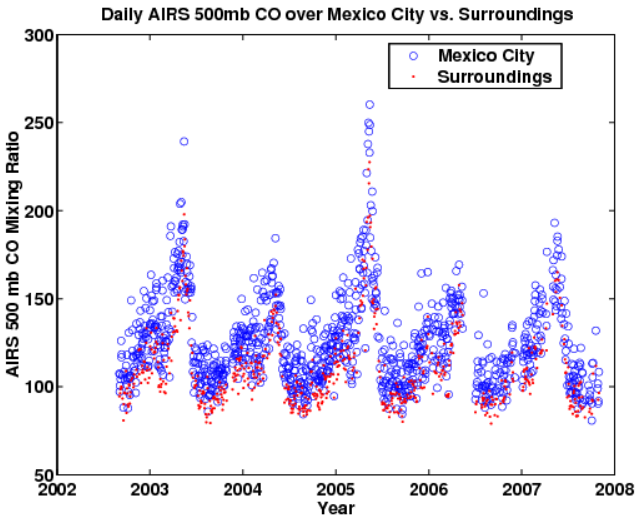

Figure 4. This timeseries shows AIRS 500 mb CO retrievals for Mexico City vs. its surrounding 1 degree grid cells.

one degree grid cells containing Mexico City is compared to the timeseries of the surrounding cells in Figure 4. Mexico City is enhanced above the background and exhibits a larger scatter. In part, AIRS sensitivity to CO over Mexico City may be due to its high altitude. Both of these timeseries show the same seasonal cycle with rather abrupt decreases in May of each year.

Larger background values around other Megacities make them less evident; however these Megacities can be seen in the AIRS CO retrievals. Five-year timeseries for six northern hemisphere Megacities in the same latitude range: New York, Los Angeles, Tokyo, Seoul, Beijing, and Tehran, have been examined. All six Megacities exhibit similar seasonal cycles but different dynamic ranges. Seoul, Tokyo, and Beijing have the highest values. Of these, Beijing presents the largest variations indicating a substantial number of polluted days at times other than the seasonal peak. Although AIRS can see anthropogenic emissions from these and other Megacities, the broad vertical sensitivity indicated by the averaging kernels means AIRS retrievals generally underestimate the near surface abundances.

5. INDONESIAN CLIMATOLOGY

A quasi-biennial variation in CO over Indonesia in October is plainly evident in the monthly average AIRS CO maps presented in Figures 5 for 2002, 2003, 2004, 2005, 2006, and 2007. Maximum values of CO over the Maritime continent occur in 2002, 2004, and 2006, with minima in 2003, 2005, and 2007. More careful examination reveals subtle differences in the CO spatial patterns for each of the peak years. Interannual variations are visible for other geographic regions, but none is as pronounced or regular during these six years as those over Indonesia.

Previous investigations have linked the variation in Indonesian CO emissions to changes in rainfall linked to El Nino.[14,46] Figures 6 show the correlation of low rainfall over Indonesia with the Southern Oscillation Index (SOI). Sustained negative values of the SOI are well known to correlate with the occurrence of El Nino.[47] The rainfall data is from the Global Precipitation Climatology Project (GPCP) monthly database[48] and the SOI data are from the Australian Bureau of Meteorology. In particular, we find that the October rainfall anomaly (specific year October rainfall minus the 10 year average October rainfall) is strongly correlated with the October SOI. For reference, 1997 marked a record strong El Nino, record drought in Indonesia, and historically large biomass burning across the Maritime continent.[14] The subtle differences between the peak burning years of 2002, 2004, and 2006, see Figure 5, indicate differences in rainfall patterns across the region as well as differences in transport patterns. Detailed

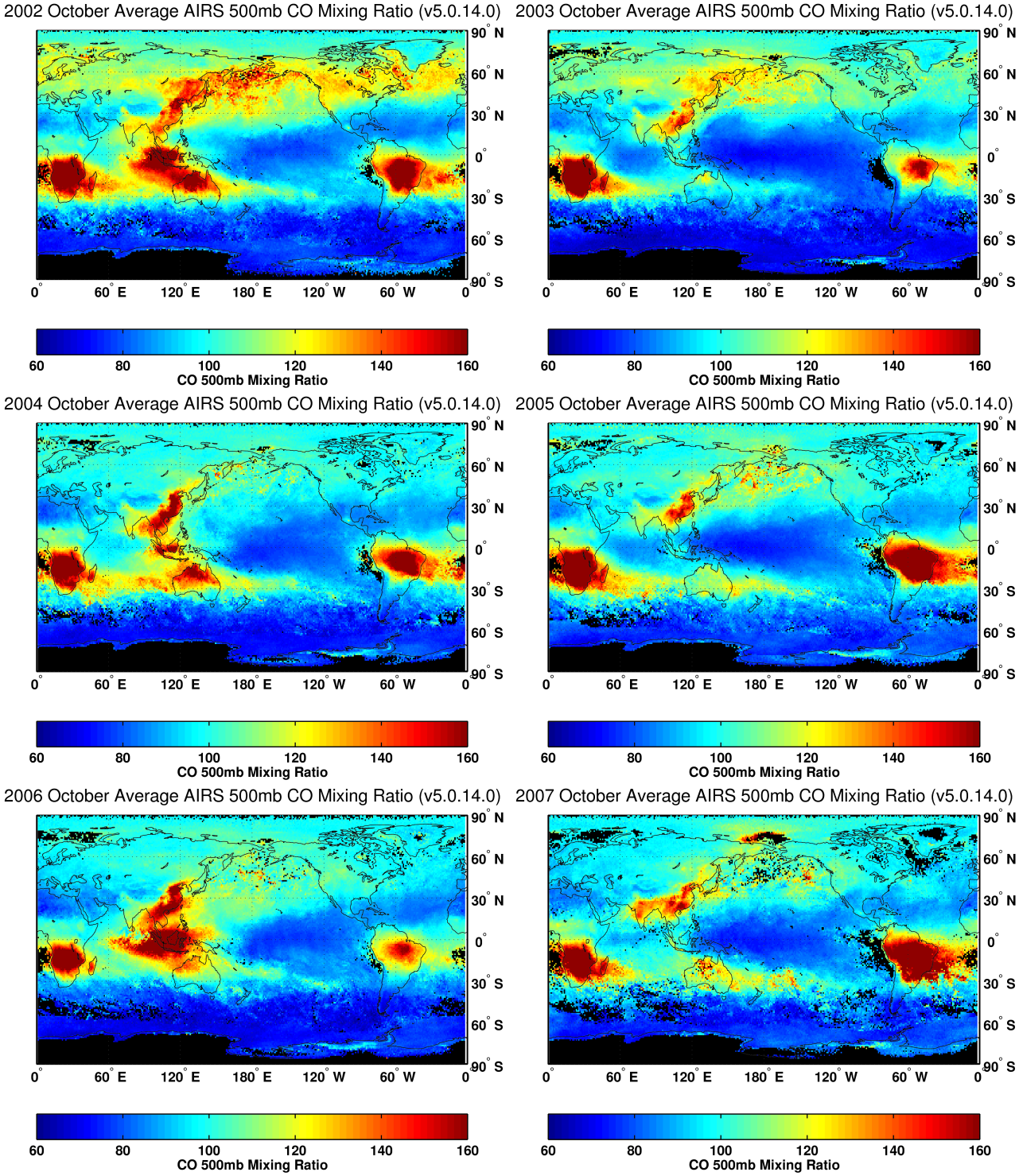

Figure 5. The six maps illustrate the average AIRS 500 mb CO for October of 2002, 2003, 2004, 2005, 2006, and 2007, respectively.

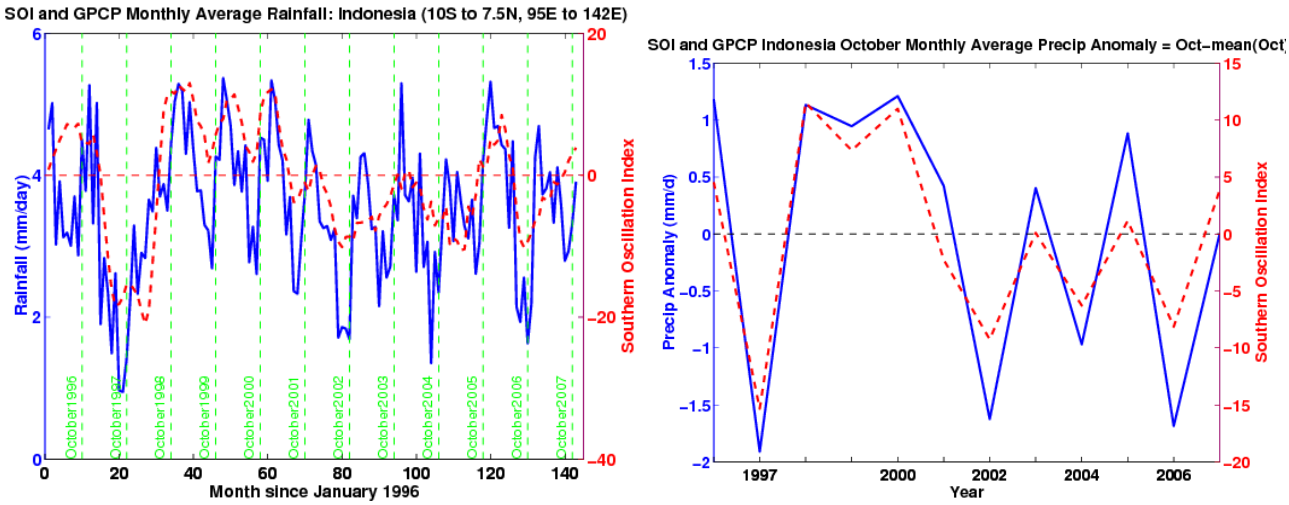

Figure 6. At left, monthly average Indonesian rainfall (10S to 7.5N, 95E to 142E), solid line, shows some correlation with the SOI, dashed line. At right, the Indonesian October precipitation anomaly is strongly correlated with the SOI.

investigations of these interannual variations in emissions and changes in transport patterns using AIRS observations and global chemical transport models are underway.

6. CONCLUSIONS

As demonstrated here, AIRS' daily views of tropospheric CO across the entire globe enable detailed analyses of both the spatial and temporal variations in emissions and the visualization of subsequent transport. We have just begun to investigate the wealth of information contained in the more than five years, and growing, of AIRS data. Recent upgrades to the AIRS CO retrieval algorithm, v5, have improved both the sensitivity to lower tropospheric CO and, most crucially, the characterization of the vertical distribution of CO information in the AIRS retrievals. The cases presented here show AIRS capabilities to see Megacites and large-scale interannual variations in emissions linked to El Nino. Ongoing analyses combining AIRS CO observations with chemical transport and inverse models will yield new insights on emission sources and dynamical mixing during long-range transport. Extending the AIRS CO record with measurements from the European IASI instrument will enable construction of a decade or longer time-series necessary for investigations of climatological variations in CO emissions and their impact on tropospheric health.

ACKNOWLEDGMENTS

The authors gratefully acknowledge support from the NASA EOS Program; through NASA grants NAG5-11163, NAG5-11653, NNG04GN42G, and NNG06GB06G and NOAA's Global Carbon Cycle Program through NOAA grant NA04AOAR4310095. Special thanks to the entire AIRS Team. WWM thanks Rae Force for her patient support. AIRS CO data is available upon request and online.

REFERENCES

[1] Chahine, M., Pagano, T. S., Aumann, H. H., Atlas, R., Barnet, C., Chen, L., Fetzer, E. J., Goldberg, M., Irion, W. F., Lambrightsen, B. H., Lee, S. Y., Lemarshall, J., McMillan, W. W., McMillin, L., Olse, E. T., Strow, L. L., and Sussking, J., "The Atmospheric InfraRed Sounder (AIRS): Providing new insights into weather and climate for the 21st Century," *Bull. Amer. Meteor. Soc.* **87**, 911–926 (2006).

[2] McMillan, W. W., Warner, J. X., Comer, M. M., Maddy, E., Chu, A., Sparling, L., Eloranta, E. W., Hoff, R. M., Sachse, G., Barnet, C., Razenkov, I. A., and Wolf, W., "Airs views of transport from 12-22 july 2004 alaskan/canadian fires: Correlation of airs co and modis aod with forward trajectories and comparison of airs co retrievals with dc-8 in situ measurements during intex-a/icartt," *J. Geophys. Res.* , submitted (2007).

[3] Thompson, A., Stone, J. B., Witte, J. C., Miller, S. K., Oltmans, S. J., Kucsera, T. L., Merrill, J. T., Forbes, G., Tarasick, D. W., Joseph, E., Schmidlin, F. J., McMillan, W. W., Warner, J., Hintsa, E. J., and Johnson, J., "IONS-04 (INTEX Ozonesonde Network Study, 2004). 2 tropospheric ozone budgets and variability over northeastern North America," *J. Geophys. Res.* **112** (2007). doi:10.1029/2006JD007670.

[4] Warner, J., McCourt, M., Barnet, C., McMillan, W. W., Wolf, W., Maddy, E., and Sachse, G., "A comparison of satellite tropospheric carbon monoxide measurments from AIRS and MOPITT during INTEX-NA," *J. Geophys. Res.* **112** (2007). doi:10.1029/2006JD007925.

[5] Morris, G., Hersey, S., Thompspn, A., Pawson, S., Nielsen, E., Colarco, P., McMillan, W., Stohl, A., Turquety, S., Warner, J., Johnson, B., Kucsera, T., Larko, D., Oltmans, S., and Witte, J., "Alaskan and Candian forest fires exacerbate ozone pollution over houston, texas on 19 and 20 july 2004," *J. Geophys. Res.* (2006). doi:101029/2006JD007090.

[6] Stohl, A., Berg, T., Fjaeraa, A., Forster, C., Herber, A., Lunder, C., McMillan, W., Oltmans, S., Solberg, S., Stebel, K., Strom, J., Torseth, K., and Yttri, K., "Arctic smoke record air pollution levels in the European Arctic during a period of abnormal warmth, due to agricultural fires in Eastern Europe," *Atmos. Chem. Phys.* **7**, 511–534 (2007).

[7] Stohl, A., Forster, C., Huntrieser, H., McMillan, W., Petzold, A., Schlager, H., and Weinzierl, B., "Aircraft measurements over Europe of an air pollution plume from Southeast Asia aerosal and chemical characterization," *Atmos. Chem. Phys.* **7**, 913–937 (2007).

[8] Logan, J. A., Prather, M. J., Wofsy, S. C., and McElroy, M. B., "Tropospheric chemistry: A global perspective," *J. Geophys. Res.* **86**, 7210–7254 (1981).

[9] Thompson, A. M., Pickering, K. E., Dickerson, R. R., Ellis, W. G., Jacob, D. J., Scala, J. R., Tao, W., McNamara, D. P., and Simpson, J., "Convective transport over the central United States and its role in regional CO and ozone budgets," *J. Geophys. Res.* **99**, 18703–18711 (1994).

[10] Hannan, J., Fuelberg, H., Crawford, J., Sachse, G., and Blake, D., "Role of wave cyclones in transporting boundary layer air to the free troposphere during the spring 2001 NASA/TRACE-P experiment," *J. Geophys. Res.* **108**(20) (2003). doi:10.1029/2002JD003105.

[11] Novelli, P. C., Steele, L. P., and Tans, P. P., "Mixing ratios of carbon monoxide in the troposphere," *J. Geophys. Res.* **97**, 20731–20750 (1992).

[12] Parrish, D. D., Holloway, J. S., Trainer, M., Murphy, P., Forbes, G. L., and Fehsenfeld, F. C., "Export of North American ozone pollution to the North Atlantic ocean," *Science* **259**, 1436–1439 (1993).

[13] Chatfield, R. B., Vastano, J. A., Sachse, G. W., and Connors, V. S., "The great African plume from biomass burning: generalizations from a three-dimensional study of TRACE-A," *J. Geophys. Res.* **103**, 28059–28077 (1998).

[14] Duncan, B. N., Martin, R. V., Staudt, A. C., Yevich, R., and Logan, J. A., "Interannual and seasonal variability of biomass burning emissions constrained by satellite observations," *J. Geophys. Res.* **108** (2003). doi:10.1029/2002JD002378.

[15] Reichle, H. G., Beck, S. M., Haynes, R. E., Hesketh, W. D., Holland, J. A., Hypes, W. D., Orr, H. D., Sherrill, R. T., Wallio, H. A., Casas, J. C., Saylor, M. S., and Gormsen, B. B., "Carbon monoxide measurements in the troposphere," *Science* **218**, 1024–1026 (1982).

[16] Connors, V. S., Miles, T., and Reichle, H. G., "Large-scale transport of a CO-enhanced air mass from Europe to the Middle East," *J. Atmos. Chem.* **9**, 479–496 (1989).

[17] Deeter, M. N., e. a., "Operational carbon monoxide retrieval algorithm and selected results for the MOPITT instrument," *J. Geophys. Res.* **108** (2003). doi:10.1029/2002JD003186.

[18] Liu, J., Drummond, J., Li, Q., Gille, J., and Ziskin, D., "Satellite mapping of CO emission from forest fires in northwest America using MOPITT measurements," *Remote Sensing of Environment* **95**(4), 502–16 (2005).

[19] Pfister, G., Hess, P. G., Emmons, L. K., Lamarque, J. F., Wiedinmyer, C., Edwards, D. P., Petron, G., Gille, J. C., and Sachse, G. W., "Quantifying CO emissions from the 2004 Alaskan wildfires using MOPITT CO data," *Geophys. Res. Lett.* **32** (2005). doi:10.1029/2005GL022995.

[20] Emmons, L., Pfister, G., Edwards, D., Gille, J., Sachse, G., Blake, D., Wofsy, S., Gerbig, C., Matross, D., and Nedelec, P., "Measurements of pollution in the troposphere (MOPITT) validation exercises during summer 2004 field campaigns over North America," *J. Geophys. Res.* **112** (2007). doi:10.1029/2006JD007833.

[21] Turquety, S., Logan, J., Jacob, D., Hudman, R., Leung, F., Heald, C., Yantosca, R., Wu, S., Emmons, L., Edwards, D., and Sachse, G., "Inventory of boreal fire emissions for North America in 2004: Importance of peat buring and pyroconvective injection," *J. Geophys. Res.* **112**(D12S03) (2007). doi:10.1029/2006DJ007281.

[22] Edwards, D. P., Emmons, L., Hauglustaine, D., Chu, A., Gille, J., Kaufman, Y., Petron, G., Yurganov, L., Giglio, L., Deeter, M., Yudin, V., Ziskin, D., Warner, J., Lamarque, J., Francis, G., Ho, S., Mao, D., Chen, J., Grechko, E., and Drummond, J., "Observations of carbon monoxide and aerosols from the Terra satellite: Northern Hemisphere variability," *J. Geophys. Res. special issue, Global Aerosol System* **109** (2004). doi:10.1029/2004JD004727.

[23] Edwards, D. P., Emmons, L. K., Gille, J. C. Chu, A., , Attie, J.-L., Giglio, L., Wood, S. W., Haywood, J., Deeter, M. N., Massie, S. T., Ziskin, D. C., and Drummond, J. R., "Satellite-observed pollution from Southern Hemisphere biomass burning," *J. Geophys. Res.* **111** (2006). doi:10.1029/2005JD006655.

[24] McMillan, W. W., Strow, L. L., Smith, W. L., Revercomb, H. E., and Huang, H. L., "The detection of enhanced carbon monoxide abundances in remotely sensed infrared spectra of a forest fire smoke plume," *Geophys. Res. Lett.* **23**(22), 3199–3202 (1996).

[25] McMillan, W. W., McCourt, M. L., Revercomb, H. E., Knuteson, R. O., Christian, T. J., Doddridge, B. G., Hobbs, P. V., Lukovich, J. V., Novelli, P. C., Piketh, S. J., Sparling, L., Stein, D., Swap, R. J., and Yokelson, R. J., "Tropospheric carbon monoxide measurements from the Scanning High-resolution Interferometer Sounder on September 7, 2000 in southern Africa during SAFARI 2000," *J. Geophys. Res.* **108**(D13) (2003). doi:10.1029/2002JD002335.

[26] McCourt, M., McMillan, W., Ackerman, S., Holz, R., Revercomb, H., and Tobin, D., "Using the "blue-spike" to characterize biomass burning sites during SAFARI 2000," *J. Geophys. Res.* **accepted**, 5 August (2004).

[27] Jones, D., Bowman, K., Palmer, P., Worden, J., Jacob, D., Hoffman, R., Bey, I., and Yantoscal, R., "Potential of observations from the tropospheric emission spectrometer to constrain continental sources of carbon monoxide," *J. Geophys. Res.* **108** (2003). doi:10.1029/2003JD003702.

[28] de Laat, A. T. J., Gloudemans, A. M. S., Aben, I., Krol, M., Meirink, J. F., van der Werf, G. R., and Schrijver, H., "Scanning imaging absorption spectrometer for atmospheric chartography carbon monoxide total columns: Statistical evaluation and comparison with chemistry transport model results," *J. Geophys. Res.* **112** (2007). doi:10.1029/2006JD008256.

[29] Aumann, H. H., Chahine, M. T., Gautier, C., Goldberg, M. D., Kalnay, E., McMillin, L. M., Revercomb, H., Rosenkranz, P. W., Smith, W. L., Staelin, D. H., Strow, L. L., and Sussking, J., "AIRS/AMSU/HSB on the Aqua mission: Design, science objectives, data products, and processing systems," *IEEE Transactions on Geo-science Remote Sensing* **41**, 253–264 (2003).

[30] Haskins, R. and Kaplan, L., "Remote sensing of trace gases using the Atmospheric InfraRed Sounder," in [*Intl Rad. Symp.*], **QC912.3 I57**, 278–281 (1992).

[31] Susskind, J., Barnet, C. D., and Blaisdell, J. M., "Retrieval of atmospheric and surface parameters from AIRS/AMSU/HSB data in the presence of clouds," *IEEE Transactions on Geo-science Remote Sensing* **41**, 390–409 (2003).

[32] McMillan, W. W., Barnet, C., Strow, L., Chahine, M., McCourt, M., Novelli, P., Korontzi, S., Maddy, E., and Datta, S., "Daily global maps of carbon monoxide: First views from NASA's Atmospheric Ifrared Sounder," *Gephys. Res. Lett.* **32**(L11801) (2005). doi:10.1029/2004GL012821.

[33] Badr, O. and Probert, S. D., "Carbon monoxide concentration in the Earth's atmosphere," *Appl. Energy* **49**, 99–143 (1994).

[34] Yurganov, L. N., Grechko, E. I., and Dzhola, A. V., "Variations of carbon monoxide density in the total atmospheric column over russia between 1970 and 1995: Upward trend and distrubances attributed to the influence of volcanic aerosols and forest fires," *Geophys. Res. Lett.* **24**(10), 1231–1234 (1997).

[35] Parrish, D., Trainer, M., Hereid, D., Williams, E., Olszyna, K., Harley, R., Meagher, J., and Fehsenfeld, F., "Decadal change in carbon monoxide to nitrogen oxide ratio in U.S. vehicular emissions," *J. Geophys. Res.* **107** (2002). doi:10.1029/2001JD000720.

[36] Lapina, K., Honrath, R., Owen, R. C., Martin, M. V., and Pfister, G., "Evidence of significant large-scale impacts of boreal fires on ozone levels in the midlatitude northern hemisphere free troposphere," *Geophys. Res. Lett.* **33** (2006). doi:10.1029/2006GL025878.

[37] Kasischke, E. S. and Turetsky, M. R., "Recent changes in the fire regime across the north american boreal region - spatial and temporal patters of burning across canada and alaska," *Geophys. Res. Lett.* **33** (2006). doi:10.1029/2006GL025677.

[38] Tobin, D., Revercomb, H. E., Knuteson, R. O., Lesht, B. M., Strow, L. L., Hannon, S. E., Feltz, W. F., Moy, L. A., Fetzer, E. J., and Cress, T. S., "ARM site atmospheric state best estimates for AIRS temperature and water vapor retrieval validation," *J. Geophys. Res.* **111** (2006). doi:10.1029/2005JD006103.

[39] Divakarla, M. G., Barnet, C. D., Goldberg, M. D., McMillin, L. M., Maddy, E., Wolf, W., Zhou, L., and Xingpin, L., "Validation of AIRS temperature and water vapor retrievals with matched radiosonde measurements and forecasts," *J. Geophys. Res.* **111** (2006). doi:10.1029/2005JD006116.

[40] Comer, M. M., *Retrieving Carbon Monoxide Abundances from the Atmospheric InfraRed Sounder (AIRS)*, PhD thesis, University of Maryland, Baltimore County (2006).

[41] Strow, L. L., Hannon, S., De Souza-Machado, S., and Motteler, H., "Validation of the AIRS radiative transfer algorithm," in [*Optical Remote Sensing Of The Atmosphere, Optical Society Of America, 2003 Technical Digest Series*], 12–15 (2003).

[42] Maddy, E. S. and Barnet, C. D., "Vertical resolution estimates in Version 5 of AIRS operational retrievals," *IEEE Transactions on Geosci. and Rem. Sens.* , accepted (2008).

[43] Rodgers, C. D. and Connor, B., "Intercomparison of remote sounding instruments," *J. Geophys. Res.* **108**(D3) (2003). doi:10.1029/2002JD002299.

[44] Swap, R. J., Annegarn, H. J., Shuttles, J. T., King, M. D., Platnick, S., Privette, J. L., and Scholes, R. J., "Africa burning: A thematic analysis of the Southern African Regional Science Initiative (SAFARI 2000)," *J. Geophys. Res.* **108**, SAF1 (2003). doi:10.1029/2003JD003747.

[45] Freitas, S. R., Longo, K. M., and Andreae, M. O., "Impact of including the plume rise of vegetation fires in numerical simulations of associated atmospheric pollutants," *Geophys. Res. Lett.* **33**(17) (2006). doi:10.1029/2006GL026608.

[46] Logan, J. A., Megretskaia, I., Nassar, R.,] Murray, L. T., Zhang, L., Bowman, K. W., Worden, H. M., and Luo, M., "Effects of the 2006 El Nio on tropospheric composition as revealed by data from the Tropospheric Em0ission Spectrometer (TES),," *Geophys. Res. Lett.* **35**, L03816 (2008). doi:101029/2007GL031698.

[47] Wright, P. B., Wallace, J. M., Mitchel, T. P., and Deser, C., "Correlation structure of the el nino/southern oscillation phenomenon," *J. Climate* **1**(6), 609–625 (1988).

[48] Adler, R. F., Huffman, G. J., Chang, A., Ferraro, R., Xie, P., Janowiak, J., Rudolf, B., Schneider, U., Curtis, S., Bolvin, D., Gruber, A., Susskind, J., Arkin, P., and Nelkin, E., "The Version 2 Global Precipitation Climatology Project (GPCP) monthly precipitation analysis (1979-present).," *J. Hydrometeor.* **4**, 1147–1167 (2003).